Destabilization of low-n peeling modes by trapped energetic particles
G. Z. Hao, Y. Q. Liu, A. K. Wang, G. Matsunaga, M. Okabayashi, Z. Z. Mou, X. M. Qiu

Destabilization of low-n peeling modes by trapped energetic particles

G. Z. Hao, Y. Q. Liu, A. K. Wang, G. Matsunaga, M. Okabayashi et al.

Citation: Phys. Plasmas **20**, 062502 (2013); doi: 10.1063/1.4811382
View online: http://dx.doi.org/10.1063/1.4811382
View Table of Contents: http://pop.aip.org/resource/1/PHPAEN/v20/i6
Published by the American Institute of Physics.

Destabilization of low-n peeling modes by trapped energetic particles

G. Z. Hao,[1] Y. Q. Liu,[2] A. K. Wang,[1] G. Matsunaga,[3] M. Okabayashi,[4] Z. Z. Mou,[1] and X. M. Qiu[1]
[1]*Southwestern Institute of Physics, PO Box 432, Chengdu 610041, China*
[2]*Euratom/CCFE Fusion Association, Culham Science Centre, Abingdon, OX14 3DB, United Kingdom*
[3]*Japan Atomic Energy Agency, 801-1, Mukouyama, Naka, Ibaraki 311-0193, Japan*
[4]*Princeton Plasma Physics Laboratory, PO Box 451, Princeton, New Jersey 08543-0451, USA*

(Received 8 January 2013; accepted 6 May 2013; published online 18 June 2013)

The kinetic effect of trapped energetic particles (EPs), arising from perpendicular neutral beam injection, on the stable low-n peeling modes in tokamak plasmas is investigated, through numerical solution of the mode's dispersion relation derived from an energy principle. A resistive-wall peeling mode with $m/n = 6/1$, with m and n being the poloidal and toroidal mode numbers, respectively, is destabilized by trapped EPs as the EPs' pressure exceeds a critical value β_c^*, which is sensitive to the pitch angle of trapped EPs. The dependence of β_c^* on the particle pitch angle is eventually determined by the bounce average of the mode eigenfunction. Peeling modes with higher m and n numbers can also be destabilized by trapped EPs. Depending on the wall distance, either a resistive-wall peeling mode or an ideal-kink peeling mode can be destabilized by EPs. © *2013 AIP Publishing LLC*. [http://dx.doi.org/10.1063/1.4811382]

I. INTRODUCTION

In tokamak plasmas, a finite large current or current gradient at the edge can drive kink mode peaking at the plasma edge, the so-called peeling mode.[1–3] Experimental observations and numerical calculations confirm that the low-n peeling/kink modes often lead to the bursting edge-localized mode (ELM), which usually reduce the confinement performance at the plasma edge. Large ELMs can induce significant heat load onto the plasma facing components and can potentially damage the materials.[4–7]

In theory, the nonlinear evolution of peeling modes is proposed as a reason for Taylor relaxation.[8] The peeling modes may result in edge harmonic oscillations in the tokamak quiescent H-mode.[9] Recently, the stable low-n ($n = 1$) peeling mode response to external magnetic field is proposed as a candidate for resonant field amplification peaking events, observed in JET device.[10] It is shown that the response of low-n peeling mode to the external magnetic field is not sensitive to the plasma rotation nor to the kinetic effect from the thermal particles. Numerical results show that the ideal peeling modes can be completely stabilized by the separatrix with an X-point in the divertor discharge.[11] The plasma resistivity can lead to an additional instability with peeling-tearing structure in the presence of an X-point.[12] The stabilization of the peeling mode in the presence of an X-point has also been analytically studied.[13] Recently, experimental observations indicate that the energetic particles (EPs) may have strong influence on the edge instabilities of tokamak plasmas.[14]

One key assumption in this work is that there is sufficient number of EPs located near the plasma edge region, which can interact with the peeling mode. In reality (in particular in present day tokamak devices), due to the large orbit width, fast ions located near the edge are often quickly lost. Therefore, a sufficient amount of EPs can be maintained near the edge, only by a continuous flux of fast ions either from the direct neutral beam injection, or from the particles transported from the core by MHD events (e.g., fishbones or off-axis fishbones) or by background turbulences. Of course, there are also confined particles whose banana centre is located relatively farther inside the plasma, but travel across the plasma edge region due to the large orbit effect. These particles can also interact with the edge localized peeling mode.

In the present work, we carry out an analytic investigation of the stability of the ideal peeling modes in the presence of trapped EPs and a resistive wall. Drift kinetic effects of EPs on the stability of the peeling mode is studied using a formulation similar to that developed for the resistive wall mode (RWM).[15–17] It is found that a stable, ideal, low-n, high-m, peeling modes can be destabilized by trapped EPs.

The dispersion relations for the resistive-wall peeling mode and for the ideal-kink peeling mode are proposed in Sec. II. In Sec. III, the kinetic effect of trapped EPs on the resistive-wall peeling mode is studied. Section IV presents calculations of trapped EPs on the ideal-kink peeling mode. Conclusion is drawn in Sec. V.

II. ANALYTIC FORMULATIONS

Since the peeling mode is localized near the plasma edge, a resistive wall has limited effect on the stability of the mode, unless the wall is located very close to the plasma boundary. In the latter case, we have an effectively RWM, which we call the resistive-wall peeling mode. If the wall is located beyond the marginal point of the ideal-wall ideal kink-peeling instability, we have an effectively ideal kink mode, but strongly localized near the plasma boundary. In the following, we consider these two cases separately. We begin with the resistive-wall peeling mode case.

A. Dispersion relation for the resistive-wall peeling mode

The dispersion relation of the resistive-wall peeling mode, including the kinetic contribution from trapped EPs, can be written as[15–21]

$$D(\omega) = -i\omega\tau_w^* + \frac{\delta W_f^\infty + \delta W_{K0}}{\delta W_f^b + \delta W_{K0}} = 0, \quad (1)$$

where $\omega(=\omega_r + i\gamma)$ is the complex frequency of the mode. For a circular cylinder, $\tau_w^* = \mu_0\sigma bd(1-a^{2m}/b^{2m})/(2m)$ defines the typical wall time of a thin resistive wall ($b \gg d$), with μ_0, a, b, d, σ, and m being the permeability of free space, the plasma minor radius, the wall minor radius, the wall thickness, the wall conductivity, and the poloidal mode number, respectively.[22] Even though only a geometrically thin wall condition is listed here, we generally require that the wall is also electromagnetically thin for our model, i.e., that the wall thickness is much smaller than the skin depth of the magnetic perturbation with a given frequency. The thin wall limit requires $d/b \ll |\omega|\tau_w \ll b/d$ with $\tau_w = \mu_0\sigma bd$. δW_f^∞ and δW_f^b represent the perturbed fluid potential energies (including contribution from vacuum space) without and with an ideal wall, respectively. δW_{K0} denotes the perturbed drift kinetic potential energy due to trapped EPs, which is generally a complex quantity. In the absence of the kinetic contribution, Eq. (1) reduces to the elegant form of the RWM dispersion relation, by means of the variational principle first derived in Ref. 23. We point out that, in the present work, the typical wall time and the fluid potential energy (δW_f^∞ and δW_f^b) are obtained based on a cylindrical geometry. However, the drift kinetic energy (δW_{K0}) calculation implicitly assumes a finite toroidicty (the large aspect ratio expansion), which validates the presence of trapped particles. Strictly speaking, the results in this work are only valid at the limit of infinite aspect ratio. Nevertheless, the main objective of this work is to provide a qualitative estimate of the influence of trapped EPs on the peeling mode. More quantitatively consistent results, in realistic tokamak geometry, can be obtained using numerical codes such as MARS-K.[24] In Eq. (1), we neglect the inertial term in our dispersion relation, due to the fact that this term is normally negligible for the RWM stability (the mode's complex frequency is small compared to the Alfven frequency). The exception is the situation where the mode's stability is close to the ideal-wall marginal point. In this case, the inertia-free assumption is not anymore valid.

The real and imaginary parts of the dispersion relation (1) can be separately written as

$$\gamma\tau_w^* = \frac{(\delta W_f^b - \delta W_f^\infty)[\delta W_f^b + \mathrm{Re}(\delta W_{K0})]}{[\delta W_f^b + \mathrm{Re}(\delta W_{K0})]^2 + \mathrm{Im}(\delta W_{K0})^2} - 1, \quad (2)$$

$$\omega_r\tau_w^* = \frac{(\delta W_f{}^b - \delta W_f{}^\infty)\mathrm{Im}(\delta W_{K0})}{[\delta W_f{}^b + \mathrm{Re}(\delta W_{K0})]^2 + \mathrm{Im}(\delta W_{K0})^2}, \quad (3)$$

where $\mathrm{Re}(\delta W_{K0})$ and $\mathrm{Im}(\delta W_{K0})$ label the real and the imaginary parts of δW_{K0}, respectively.

Equation (2) implies that the stability of the mode depends on the balance between the energy components δW_f^b, $\mathrm{Re}(\delta W_{K0})$, and $\mathrm{Im}(\delta W_{K0})$. In particular, for an unstable mode, the imaginary part of the kinetic energy, $|\mathrm{Im}(\delta W_{K0})|$, always reduces the growth rate γ of the mode. On the other hand, if the fluid peeling mode is stable (e.g., $\gamma < 0$), the amplitude of the damping rate depends on the sign of $\delta W_f^b + \mathrm{Re}(\delta W_{K0})$. For a positive (negative) $\delta W_f^b + \mathrm{Re}(\delta W_{K0})$, $|\mathrm{Im}(\delta W_{K0})|$ stabilizes (destabilizes) the stable peeling mode. In all cases, $|\mathrm{Im}(\delta W_{K0})|$ can significantly affect the growth/damping rate of the peeling mode, only when $|\mathrm{Im}(\delta W_{K0})|$ is larger than or comparable to $|\delta W_f^b + \mathrm{Re}(\delta W_{K0})|$. In contrast, the growth rate of the mode is mainly determined by $\delta W_f^b + \mathrm{Re}(\delta W_{K0})$.

We consider a cylindrical plasma equilibrium with a circular cross section and a flat plasma density $\rho(r) = \rho_0$.[20,25] In the cylindrical coordinates ($\mathbf{e}_r$, $\mathbf{e}_\theta$, $\mathbf{e}_z$), the equilibrium current, magnetic field, and plasma pressure are assumed as $\mathbf{J} = J_0\mathbf{e}_z$, $\mathbf{B} = B_0\mathbf{e}_z + B_\theta\mathbf{e}_\theta$, and $P = P_0(1-r^2)$, respectively, with $B_\theta = \mu_0 J_0 r/2$ inside the plasma and $P_0 = \mu_0 J_0^2/4$ being the plasma pressure at the magnetic axis. The above cylindrical model gives a flat q(the safety factor) profile. For the given equilibrium, the perpendicular component of the mode displacement is taken as $\boldsymbol{\xi}_\perp = \frac{m\psi_0}{Fa}(\mathbf{e}_r + i\mathbf{e}_\theta)\hat{r}^{m-1}e^{i(m\theta-n\phi)}$ with $F = (m-nq)B_0/(Rq)$ and $\hat{r} = r/a$, where r, R, θ, ϕ, and n are the radial coordinate, the plasma major radius, the poloidal angle, the toroidal angle, and the toroidal mode number, respectively. Here, ψ_0 labels the perturbed magnetic flux at the plasma edge. Given the mode eigenfunction, the perturbed drift kinetic energy, δW_{K0}, for a large aspect ratio toroidal plasma, can be calculated as shown in Sec. II C. We emphasize that our calculations for the peeling mode stability is strictly consistent only at infinite aspect ratio limit. Nevertheless, we follow this approach for finite aspect ratio cases, aiming at qualitative study of the kinetic effect of EPs on the peeling mode stability. Here we write down the fluid potential energy perturbations, which are normalized to $\pi\psi_0^2 B_0^2 m^2/2R\mu_0 F^2$. The normalized forms of the fluid potential energy, without and with an ideal wall (at the minor radius b), are given, respectively, as[1,20]

$$\delta W_f^\infty = -4\pi\frac{(m-nq)^2}{mq^2}\left(\frac{1}{m-nq} - 1\right) \quad (4)$$

and

$$\delta W_f^b = -4\pi\frac{(m-nq)^2}{mq^2}\left[\frac{1}{m-nq} - \frac{1}{1-(b/a)^{-2m}}\right]. \quad (5)$$

Equations (4) and (5) are valid for a circular cylindrical plasma with a uniform current density.

B. Dispersion relation for the ideal-kink peeling mode

For an ideal-kink peeling mode, the plasma inertia cannot generally be neglected. In this case, the full dispersion relation should be used[17]

$$(-i\omega/\omega_{ds} - in\Omega_0)^2\delta K + \delta W_p + \frac{\delta W_V^\infty - i\omega\tau_w^*\delta W_V^b}{1 - i\omega\tau_w^*} + \delta W_{K0} = 0, \quad (6)$$

where $\Omega_0 \equiv \omega_0/\omega_{ds}$ is the plasma rotation frequency, normalized by the toroidal precession drift frequency of energetic particles at the birth energy $\omega_{ds} = (2\mathrm{E} - \mathrm{K})qE_m/(\mathrm{K}\omega_c rR)|_{r=a}$.

Here, E_m and ω_c are the birth energy of the trapped EPs and the cyclotron frequency of the trapped EPs, respectively. K and E are the complete elliptic integrals of the first and second kinds, respectively. The normalized inertial term δK, the perturbed potential energy of the bulk plasma δW_p, the perturbed magnetic energy in the vacuum with an ideal wall (δW_V^b) and without wall (δW_V^∞) are given, respectively, as[26]

$$\delta K = \frac{2\pi}{m}\tau_A^2\omega_{ds}^2, \tag{7}$$

$$\delta W_p = -4\pi\frac{(m-nq)^2}{mq^2}\left(\frac{1}{m-nq}-\frac{1}{2}\right), \tag{8}$$

$$\delta W_V^b = 4\pi\frac{(m-nq)^2}{mq^2}\frac{1+(b/a)^{-2m}}{2[1-(b/a)^{-2m}]}, \tag{9}$$

and

$$\delta W_V^\infty = 2\pi\frac{(m-nq)^2}{mq^2}, \tag{10}$$

where $\tau_A \equiv R\sqrt{\mu_0\rho_0}/B_0$.

Note that the sum of the perturbed plasma potential energy, Eq. (8), and the no-wall vacuum energy, Eq. (10), recovers the total fluid energy without wall, Eq. (4). Similarly, Eq. (5) is recovered by the sum of Eqs. (8) and (9), in the presence of an ideal wall. When the resistive wall is placed at infinity, Eq. (6) converts to the following dispersion relation for an ideal kink mode, including the kinetic effect from trapped EPs:

$$(-i\omega/\omega_{ds} - in\Omega_0)^2\delta K + \delta W_p + \delta W_V^\infty + \delta W_{K0} = 0. \tag{11}$$

For an ideal kink mode (in our case, the kink-peeling mode), the effect of the resistive wall is normally negligible. This motivates our choice of the dispersion relation (11) for the kink-peeling branch.

Separating the above equation into the imaginary and real parts, we obtain two equations

$$\gamma = \frac{\mathrm{Im}(\delta W_{K0})}{2(\Omega_r + n\Omega_0)\delta K}\omega_{ds} \tag{12}$$

and

$$(\Omega_r+n\Omega_0)^2 - \frac{[\mathrm{Im}(\delta W_{k0})]^2}{4(\Omega_r+n\Omega_0)^2\delta K} - \frac{\delta W_p+\delta W_V^\infty+\mathrm{Re}(\delta W_{K0})}{\delta K} = 0, \tag{13}$$

where $\Omega_r = \omega_r/\omega_{ds}$. Equation (12) indicates that the growth rate of the ideal kink-peeling mode is proportional to $\mathrm{Im}(\delta W_{k0})$, but is inversely proportional to the real frequency of the mode in the plasma frame. Since both the mode growth/damping rate and frequency is unknown, Eq. (12) is a nonlinear equation for the mode eigenvalue. It is worthwhile to note that the sign of the mode growth rate (stable or unstable) depends on the sign of the imaginary part of the drift kinetic energy perturbation, as well as on the sign of the Doppler-shifted mode frequency. Equation (12) is valid only when the contribution of the trapped EPs is included in the ideal-kink peeling mode dispersion relation. In the absence of the trapped EPs (i.e., $\delta W_{K0} = 0$), Eq. (11) cannot be rewritten as Eqs. (12) and (13) anymore, and it reduces to

$$(-i\omega/\omega_{ds} - in\Omega_0)^2\delta K + \delta W_p + \delta W_V^\infty = 0. \tag{14}$$

Then, the mode's complex frequency relates to the sign of $\delta W_p + \delta W_V^\infty$, when $\delta W_p + \delta W_V^\infty > 0$, there exists a marginally stable mode with real frequency $\Omega_r = \pm\sqrt{(\delta W_p + \delta W_V^\infty)/\delta K} - n\Omega_0$; when $\delta W_p + \delta W_V^\infty < 0$, there is an unstable/stable mode with growth/damping rate $\gamma = \pm\omega_{ds}\sqrt{|\delta W_p + \delta W_V^\infty|/\delta K}$, real frequency $\Omega_r = -n\Omega_0$.

Equation (13) can be further written as

$$(\Omega_r + n\Omega_0)^2 = \frac{1}{\delta K}\frac{[\delta W_p + \delta W_V^\infty + \mathrm{Re}(\delta W_{K0})] + \sqrt{[\delta W_p + \delta W_V^\infty + \mathrm{Re}(\delta W_{K0})]^2 + [\mathrm{Im}(\delta W_{K0})]^2}}{2}. \tag{15}$$

Note that, if $\mathrm{Im}(\delta W_{K0}) = 0$, the quadratic dispersion relation (11) predicts an either purely growing mode, or a marginally stable mode with a finite real frequency. No other branches are possible. Depending on the sign of $\mathrm{Im}(\delta W_{K0})$, either a growing or a damping mode can exist, with finite mode frequency determined by Eq. (15).

C. Calculation of the drift kinetic energy δW_{K0} due to EPs

In the case of neutral beam injection heating, the pitch angle of the trapped EPs is determined by the magnetic field at the ionization position and the injection angle of the beam. In the large aspect ratio approximation, all of the trapped EPs have the same pitch angle $\lambda = v_\perp^2 B_0/v^2 B$, with v and $v_\perp$ being the total velocity and perpendicular velocity of EPs, respectively. Due to the drag effect of the background electrons, the trapped EPs' normalized distribution function depends on the EPs' energy as a form $f \propto E^{-1}$, where $E = v^2/2$ is the kinetic energy (with the particle mass normalized to unity). The normalized distribution function, with a single pitch angle, is written as[27]

$$f \sim n_0\delta(\lambda - \lambda_0)E^{-1}, \tag{16}$$

where n_0 is a constant related to the radial density of EPs. $B = B_0(1 - r\cos\theta/R)$ is the toroidal magnetic field in the plasma (with a large aspect ratio approximation). Following a similar derivation as presented in Ref. 27, the normalized perturbed kinetic energy from trapped EPs is calculated

$$\delta W_{K0}=\frac{12\pi\beta\beta^*(1-\lambda_0/2)^2}{\mathrm{K}(1-\hat{r}_{\min}^{3/2})}\frac{R}{a}[\Omega(\tilde{A}\Xi_1-\tilde{B}\Xi_3)+\tilde{C}\Xi_2], \quad (17)$$

where $\Omega=(\omega-\omega_0)/\omega_{ds}$ and $\hat{r}_{\min}=|1-1/\lambda_0|R/a$. Here ω_0 is the plasma rotation frequency. A key parameter is introduced here $\beta*=\beta_h/\beta$ as the normalized beta of EPs, with β and β_h being the volume averaged bulk plasma pressure and the EPs' (hot ion's) pressure, respectively, normalized by the magnetic pressure. In the present tokamak devices (e.g., DIII-D and JT-60U), β^* is in the order of the inverse aspect ratio a/R. However, in the future ITER operational parameter regime, β^* will exceed current experiment. In this work, we assume that the density of the EPs is much smaller than the bulk MHD density, but the EPs β_h is in the order of the bulk plasma β (i.e., $\beta^*\sim 1$).[28]

To obtain Eq. (17), only the precessional drift resonance of trapped hot ions with the peeling mode is included. The precession drift frequency is analytically calculated for a large aspect ratio circular plasma, and expressed via the elliptic integrals of the first (K) and the second (E) kinds, respectively, with the argument $k_t^2=(1-\lambda+\lambda\epsilon)/2\lambda\epsilon$. We point out a major difference in the derivation of δW_{K0}, compared with that from Ref. 27: in this work, the eigenfunction of the mode is assumed to be edge localized peeling mode, requiring a choice of high m poloidal mode number. In fact, our derivation here assumes an arbitrary poloidal harmonic number, though certain simplifications can be achieved at the large m limit, as will be shown soon. The factors Ξ_1, Ξ_2, and Ξ_3 in Eq. (17) are defined as

$$\begin{aligned}\Xi_1=&\frac{1}{2(m-1)+1/2}\hat{r}^{2(m-1)+1/2}\ln\left(1-\frac{1}{\Omega\hat{r}}\right)\Big|_{\hat{r}_{\min}}^{1}\\&-\frac{1}{2(m-1)+1/2}\\&\times\left\{2\sqrt{\hat{r}}\sum_{k=0}^{2(m-1)-1}\frac{\hat{r}^{2(m-1)-1-k}}{\{2[2(m-1)-1]-2k+1\}\Omega^{k+1}}\Big|_{\hat{r}_{\min}}^{1}\right.\\&\left.-\Omega^{-2(m-1)-1/2}\ln\frac{1+\sqrt{\Omega\hat{r}}}{1-\sqrt{\Omega\hat{r}}}\Big|_{\hat{r}_{\min}}^{1}\right\}, \quad (18)\end{aligned}$$

$$\Xi_2=\frac{1}{2(m-1)+1/2}\left(1-\hat{r}_{\min}{}^{2(m-1)+1/2}\right), \quad (19)$$

$$\begin{aligned}\Xi_3=&2\sqrt{\hat{r}}\sum_{k=0}^{2(m-1)}\frac{\hat{r}^{2(m-1)-k}}{[2(2m-2)-2k+1]\Omega^{k+1}}\Big|_{\hat{r}_{\min}}^{1}\\&+\Omega^{-2(m-1)-3/2}\ln\frac{1+\sqrt{\Omega\hat{r}}}{1-\sqrt{\Omega\hat{r}}}\Big|_{\hat{r}_{\min}}^{1}. \quad (20)\end{aligned}$$

Similar to the classical fishbone theory, the imaginary part of the drift kinetic energy, $\mathrm{Im}(\delta W_{K0})$, mainly arises from the log-functions in Ξ_1 and Ξ_3. These log-functions reflect the mode-particle resonance, and eventually contribute to the complex frequency of the mode. At the marginal stability point ($\gamma=0$), $\mathrm{Im}(\delta W_{K0})$ is solely induced by the mode-particle resonance. The other coefficients $\tilde{A}$, $\tilde{B}$, and $\tilde{C}$ in Eq. (17) are functions of the particle pitch angle λ_0 only. They are defined/calculated by the following set of formulae:

$$\tilde{A}=\left[\hat{A}-\hat{B}+(\hat{D}-2\hat{C})\frac{2\mathrm{E}-\mathrm{K}}{\mathrm{K}q}\right]_{\hat{r}=1}, \quad (21)$$

$$\tilde{B}=\left(\hat{B}+\hat{C}\frac{2\mathrm{E}-\mathrm{K}}{\mathrm{K}q}\right)_{\hat{r}=1}, \quad (22)$$

$$\tilde{C}=\left[(\hat{D}-\hat{C})\frac{2\mathrm{E}-\mathrm{K}}{\mathrm{K}q}\right]_{\hat{r}=1}, \quad (23)$$

$$\hat{A}=-\frac{\mathrm{K}}{2\lambda_0}\Lambda_1-\frac{1}{2\lambda_0}\Lambda\frac{\partial\mathrm{K}}{\partial k_t{}^2}, \quad (24)$$

$$\hat{B}=-\frac{1}{\lambda_0}\frac{\mathrm{K}^2\Lambda}{2\mathrm{E}-\mathrm{K}}\frac{\partial}{\partial k_t{}^2}\left(\frac{\mathrm{E}}{\mathrm{K}}\right), \quad (25)$$

$$\hat{C}=\frac{\mathrm{K}\Lambda}{2\mathrm{E}-\mathrm{K}}\left[(1-2k_t{}^2)\mathrm{K}\frac{\partial}{\partial k_t{}^2}\left(\frac{\mathrm{E}}{\mathrm{K}}\right)-(2\mathrm{E}-\mathrm{K})\right], \quad (26)$$

$$\begin{aligned}\hat{D}=&\left(\frac{1-2k_t{}^2}{2}\Lambda_1\mathrm{K}-\frac{1}{2}\Lambda\mathrm{K}+\frac{1}{2}(1-2k_t{}^2)\Lambda\frac{\partial\mathrm{K}}{\partial k_t{}^2}\right)\\&+\Lambda\mathrm{K}(2m-2). \quad (27)\end{aligned}$$

In the drift kinetic calculations, the peeling mode eigenfunction eventually enters into δW_{K0} in the bounce averaged form (shown by the top bar below), via the following factors:

$$\Lambda=\overline{\cos\hat{m}\theta}^2=\left[\frac{I}{\sqrt{2}\mathrm{K}(k_t^2)}\right]^2, \quad (28)$$

$$\Lambda_1=\frac{\partial}{\partial k_t^2}\overline{\cos\hat{m}\theta}^2=\sqrt{2}\overline{\cos\hat{m}\theta}\frac{I'\mathrm{K}-I\mathrm{K}'}{\mathrm{K}^2}, \quad (29)$$

where $\hat{m}=m-1$.

At sufficiently large $\hat{m}$, the factor I, as well as its derivative I' with respect to k_t^2, can be well approximated by analytic formulae shown below

$$I=\int_0^{\theta_b}\frac{\cos\hat{m}\theta d\theta}{(\cos\theta-\cos\theta_b)^{1/2}}\approx 2^{4/5}\frac{\cos\left(\hat{m}\theta_b-\frac{\pi}{4}\right)}{\sqrt{\hat{m}\sin\theta_b}} \quad (30)$$

and

$$I'\approx\frac{-2^{4/5}\left[\sin\left(\hat{m}\theta_b-\frac{\pi}{4}\right)\hat{m}\sqrt{\sin\theta_b}+\cos\left(\hat{m}\theta_b-\frac{\pi}{4}\right)\cos\theta_b/2/\sqrt{\sin\theta_b}\right]}{k_t\sqrt{\hat{m}}\sin\theta_b\cos\frac{\theta_b}{2}}, \quad (31)$$

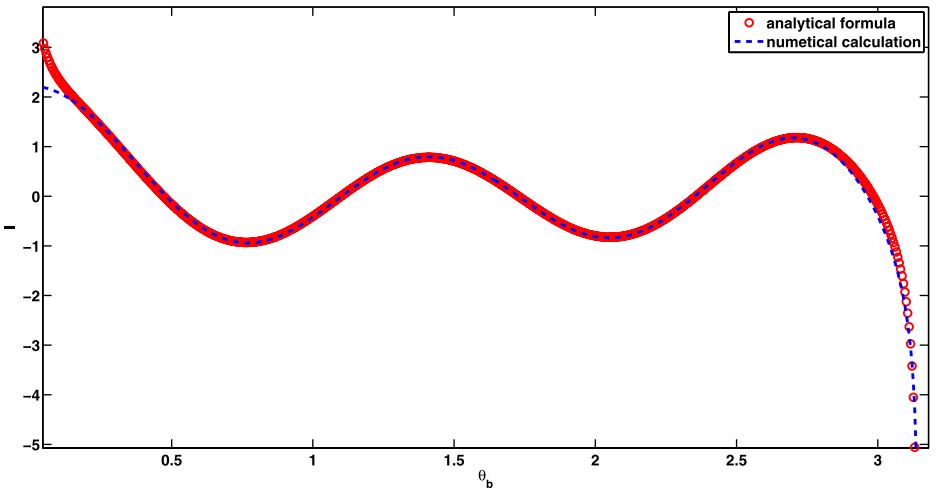

FIG. 1. Comparison of the numerically computed (dashed line) and analytically approximated (solid line) factor I, defined in Eq. (30) and associated with the bounce average of the peeling mode eigenfunction. θ_b is the poloidal angle of the turning point of the trapped banana orbit. Shown is a case with $\hat{m} = 5$.

where $\theta_b = 2\arcsin(k_t)$ denotes the poloidal angle of the turning point of trapped EPs. The above approximation significantly facilitates the analytic calculation of the kinetic energy δW_{K0}. Numerical evaluation of the integral in Eq. (30) confirms the accuracy of the analytic approximation at high $\hat{m}$. One example is shown in Fig. 1 for $\hat{m} = m - 1 = 5$. Except for the regions near the boundaries of θ_b (i.e., $\theta_b = 0$ and $\theta_b = \pi$), the analytical approximation re-produces very well the numerical results. Note that we have precisely treated the singularity point $\theta = \theta_b$ in the numerical integration. The periodic behavior of I versus θ_b is due to the bounce average of $\cos\hat{m}\theta$, which is a periodic function of θ_b for a given $\hat{m}$. In the present study, the value of θ_b is in a range from 0.2 to 2.2. In this range, the analytic approximation, Eq. (30), is reliable.

III. DESTABILIZATION OF RESISTIVE-WALL PEELING MODE BY EPs

We numerically solve the normalized form of the dispersion relation (1), choosing the following parameters $m = 6$, $n = 1$, $a = 1\,\mathrm{m}$, $R = 3\,\mathrm{m}$, $B_0 = 2.3\mathrm{T}$. The EPs' birth energy is $E_b = m_h E_m = 85\,\mathrm{KeV}$. The value of the safety factor, which is a constant in our analytic equilibrium model, is $q = 6.05$. A close-fitting wall is located at $b = 1.05a$, resulting in a resistive-wall peeling mode. The wall conductivity is assumed to be $\sigma = 10^6\Omega^{-1}\,\mathrm{m}^{-1}$, and the wall thickness is $d = 0.01a$. The plasma density is $n_0 = 10^{20}\,\mathrm{m}^{-3}$. Here, m_h denotes the mass of EPs. These plasma and wall parameters are chosen mainly to have a fluid-wise stable peeling mode in the absence of kinetic effects. In particular, the choice of the harmonic numbers and the (flat) q value yields positive (i.e., stable) fluid potential energy both with and without an ideal wall, with $\delta W_f^\infty = 0.003 > 0$ and $\delta W_f^b = 0.0032 > 0$. We note that δW_f^b is only slightly larger than δW_f^∞, indicating a weak stabilization effect of the ideal wall on a stable peeling mode. Because the peeling mode has a large poloidal number, the field perturbation, caused by the mode, decays fast in the vacuum region outside the plasma. Therefore, the wall can hardly provide a significant influence on the peeling mode stability, unless the wall is placed very close to the plasma boundary. Even though our analytic calculations assume a large aspect ratio approximation, we choose typical parameter ranges corresponding to a conventional tokamak plasma, bearing in mind that the results presented in this work provide more qualitative than quantitative conclusions. The birth energy of the EPs follows typical values in the present day devices with neutral beam injections.

Figure 2 plots the normalized growth rate and the real frequency of the resistive-wall peeling mode as a function of the normalized EPs' beta β^*. Note that we assume a finite plasma rotation frequency here, with $\Omega_0 = -1.8$. This rotation frequency (as well as the real frequency of the peeling mode) is normalized by the nominal precession frequency of trapped EPs. This rotation frequency corresponds to a value of 3.6%, when normalized by the Alfven frequency.

Since δW_f^b and δW_f^∞ are both positive, at $\beta^* = 0$(without the kinetic effect from trapped EPs), the peeling mode is stable. With increasing β^*, the initially stable peeling mode becomes less stable, approaching the marginal stability as the normalized beta approaches a threshold value. As the beta value exceeds the threshold ($\beta^* > \beta_c^* = 0.445$), the peeling mode enters into the unstable domain. And the growth rate of the mode slowly increases with β^*. This shows that trapped EPs can destabilize a stable peeling mode at a sufficient fraction of hot ion pressure. It is worth to point out that the mode's frequency, including the below results in this section, keeps consistent with the thin wall assumption, which is an important assumption to obtain dispersion relation (Eq. (1)). We also mention that, in order to obtain a continuous crossing of the eigenvalue through the marginal stability, the phase of log-functions from Eqs. (18) and (20) is defined in the range of -3π to π.

The destabilization of the peeling mode can be understood in terms of the drift kinetic energy perturbation. As shown in Fig. 3(a), the $\mathrm{Re}(\delta W_{K0})$ is negative and its amplitude increases with β^*, resulting in a decrease of $\mathrm{Re}(\delta W_{K0}) + \delta W_f^\infty$. At the marginal point $\beta^* = \beta_c^*$, $\mathrm{Re}(\delta W_{K0})$ roughly equals to $\sim -\delta W_f^\infty$, and $|\mathrm{Im}(\delta W_{K0})|$ is much smaller than $|\mathrm{Re}(\delta W_{K0}) + \delta W_f^b|$ as shown in Fig. 3(b). Therefore, near the marginal point β_c^*, Eq. (2) can be approximately written as

$$\gamma\tau_w^* = -\frac{\delta W_f^\infty + \mathrm{Re}(\delta W_{K0})}{\delta W_f^b + \mathrm{Re}(\delta W_{K0})}, \tag{32}$$

which implies that an instability can occur if $\mathrm{Re}(\delta W_{K0})$ is in the region from $-\delta W_f^b$ to $-\delta W_f^\infty$, with $-\delta W_f^b = -0.0032$

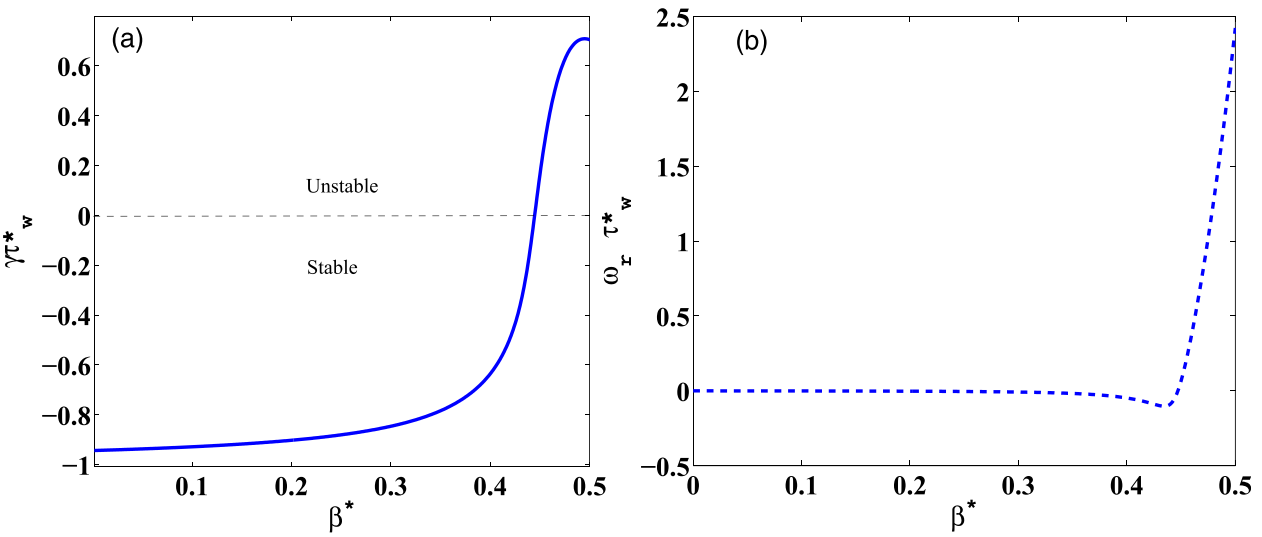

FIG. 2. (a) The growth/damping rate normalized by the resistive wall time and (b) the real frequency normalized by the nominal toroidal precession frequency of trapped EPs, of the $m/n = 6/1$ resistive-wall peeling mode versus the normalized EPs pressure β^*. Other parameters are assumed as $b = 1.05a$, $q = 6.05$, $\lambda_0 = 0.99$, and $\Omega_0 = -1.8$.

and $-\delta W_f^\infty = -0.003$ for the case studied here. When $\beta * > \beta_c^*$, $|\mathrm{Im}(\delta W_{K0})|$ increases with β^*, and finally becomes comparable to $|\mathrm{Re}(\delta W_{K0}) + \delta W_f^b|$. Both the real and imaginary parts of the drift kinetic energy perturbation results in the dependence of the mode's growth rate on β^*, as the curve in the unstable domain in Fig. 2(a). In addition, calculations show that the marginal stability always occurs when $\mathrm{Re}(\delta W_{K0}) \sim -\delta W_f^\infty$ and $|\mathrm{Im}(\delta W_{K0})| \ll |\mathrm{Re}(\delta W_{K0}) + \delta W_f^b|$. Equation (3) suggests that the real frequency ω_r of the mode is proportional to $|\mathrm{Im}(\delta W_{K0})|$. In the region $\beta^* < \beta_c^*$, ω_r almost vanishes (Fig. 2(b)), due to the small value of $|\mathrm{Im}(\delta W_{K0})|$, and the dependence of denominator of Eq. (3) on β^* is mainly determined by $\mathrm{Re}(\delta W_{K0})$. In the region $\beta^* > \beta_c^*$, ω_r is roughly proportional to EPs' beta, which is determined by both $|\mathrm{Re}(\delta W_{K0})|$ and $|\mathrm{Im}(\delta W_{K0})|$.

The threshold beta value β_c^* of EPs, for destabilizing the resistive-wall peeling mode, depends on the particle pitch angle λ_0 in a complicated manner, as shown by Fig. 4(a). There are multiple windows in terms of λ_0, in which the peeling mode can be destabilized as $\beta^* > \beta_c^*$. The value of β_c^* reaches its local minimum at certain values of λ_0. This peculiar dependence of β_c^* on λ_0 is eventually due to the periodic behavior of the bounce average of the peeling mode eigenfunction with a high-m number. This is illustrated by the coefficients Λ and Λ_1 shown in Fig. 4(b). The fact that these two coefficients are periodic functions of the pitch angle λ_0 follows from the analytic estimates (30) and (31), in which the trapped particle turning point poloidal angle is directly related to λ_0. Next, we show that that this periodic behavior in Λ and Λ_1 propagates into β_c^* via the drift kinetic energy perturbation. We find that, at the marginal stability point β_c^*, $\mathrm{Im}(\delta W_{K0})$ is small and δW_{K0} is roughly equal to $\mathrm{Re}(\delta W_{K0}) \sim -\delta W_f^\infty$. Since $|\Lambda| \ll |\Lambda_1|$ as shown in Fig. 4(b), the value of δW_{K0} is mainly determined by the Λ_1 factor. Equations (17) and (21)–(27) suggest that δW_{K0} has a roughly linear dependence on Λ_1 through the terms $\tilde{A}$ and $\tilde{C}$. Therefore, at the marginal point, $\delta W_{K0} \sim -\delta W_f^\infty$ is roughly proportional to the product $\Lambda_1 \beta_c^*$. Since $-\delta W_f^\infty$ is a fluid term and thus independent of λ_0, β_c^* is roughly inversely proportional to Λ_1. The sign of Λ_1 is also important here–only a negative Λ_1 gives a negative $\mathrm{Re}(\delta W_{K0})$, which is required to cancel the positive δW_f^∞ in order to obtain a marginal stability. Put together the above discussions, as well as the dependence of $\Lambda_1(\lambda_0)$ on λ_0 as shown in Fig. 4(b), we find that the smallest β_c^* should occur at smallest (negative) Λ_1, which in turn occurs at $\lambda_0 \sim 1.01, 1.26, 1.47$. This explains the

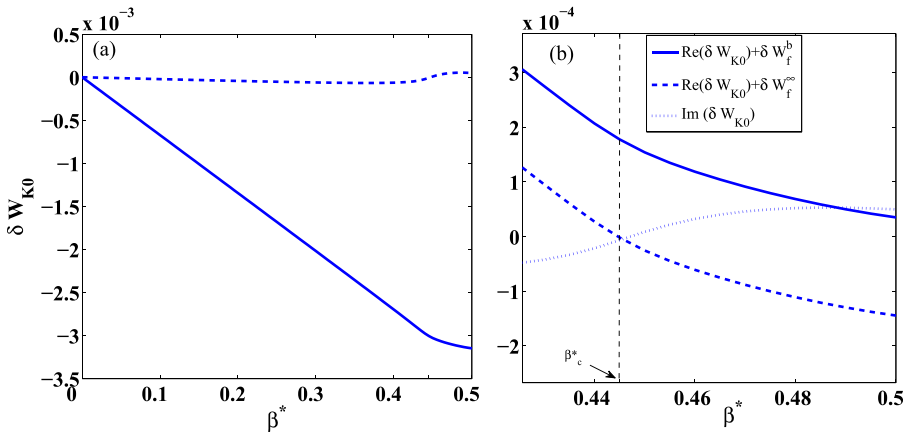

FIG. 3. (a) The $\mathrm{Re}(\delta W_{K0})$(solid line) and $\mathrm{Im}(\delta W_{K0})$ (dashed line) versus β^*; (b) the energy combinations $\mathrm{Re}(\delta W_{K0}) + \delta W_f^b$, $\mathrm{Re}(\delta W_{K0}) + \delta W_f^\infty$, and $\mathrm{Im}(\delta W_{K0})$ as functions of β^*. The vertical lines label the threshold beta value, β_c^*, for EPs. The same parameters set, $b = 1.05a$, $q = 6.05$, $\lambda_0 = 0.99$, and $\Omega_0 = -1.8$, as in Fig. 2, are used.

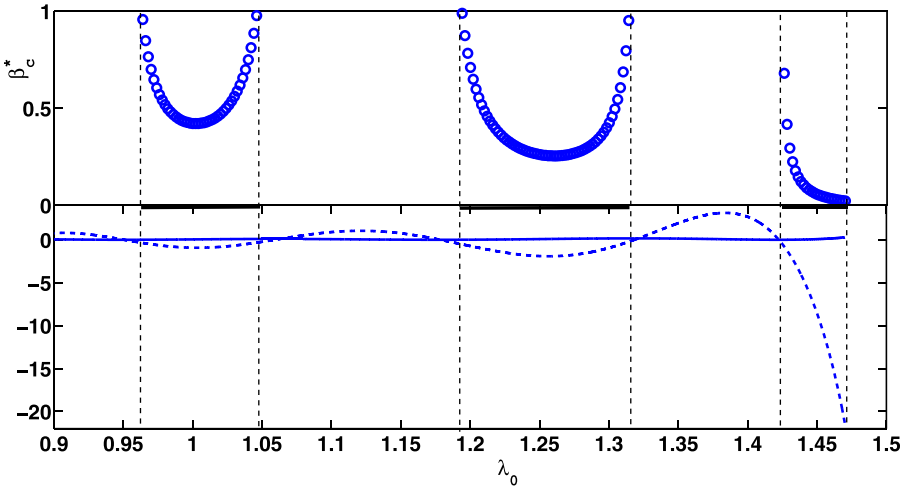

FIG. 4. (a) The threshold beta value, β_c^*, for destabilizing the resistive-wall peeling mode, as a function of λ_0; (b) the coefficients Λ (solid line) and Λ_1 (dashed line), as defined in Eqs. (28) and (29), respectively, versus the particle pitch angle λ_0. The other parameters set as in Fig. 2 are used.

local minima of $\beta_c^*(\lambda_0)$ at these values of λ_0. We point out again that the physics associated with this periodic behavior is bounce average of the peeling mode eigenfunction, with a specific poloidal periodicity $\cos(\hat{m}\theta)$.

In addition, the β_c^* rapidly increasing at some λ_0 points means that β_c^* is sensitive to the value of the EPs' pitch angle λ_0. As discussed above, β_c^* is roughly inversely proportional to the value of Λ_1. Hence, when Λ_1 approaches zero at some typical points, the value of β_c^* rapidly increases. Here, Λ_1 is related to the derivation of the bounce average of the peeling mode eigenfunction with respect to the quantity $k_t^2 = (1-\lambda+\lambda\epsilon)/2\lambda\epsilon$ as defined by Eq. (29). In fact, the rapid increase of β_c^* at some points is mainly related to the bounce average of the peeling mode eigenfunction.

We also carry out a sensitivity study of the critical beta β_c^* on the plasma equilibrium parameter q, which dictates the stability of the peeling mode in the fluid approximation. The results are shown in Fig. 5. We fix the EPs' pitch angle $\lambda_0 = 0.99$ and the plasma rotation frequency $\Omega_0 = -1.8$ as in Fig. 2. Figure 5 shows that β_c^* is roughly proportional to q. As the (edge) q value exceeds an integer number (6 in our case), the fluid peeling mode becomes more stable with increasing q. The results in Fig. 5 indicate that the excitation of a more stable resistive-wall peeling mode requires a larger fraction of trapped EPs.

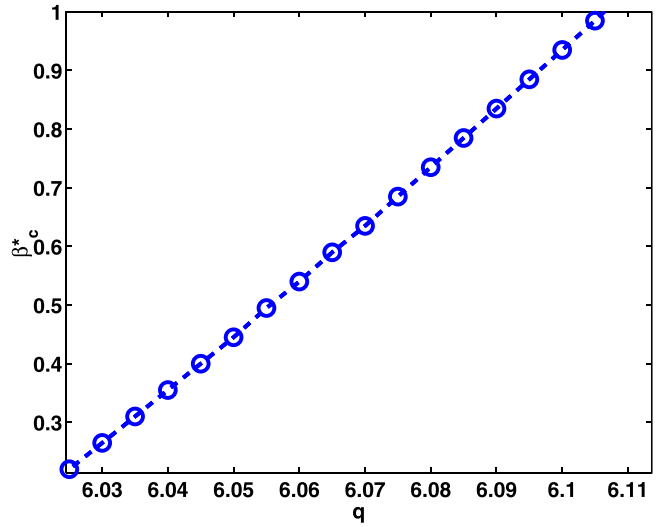

FIG. 5. The critical beta value, β_c^*, for destabilizing the resistive-wall peeling mode, versus the edge q-value. The other parameters are, $b = 1.05a$, $\lambda_0 = 0.99$, and $\Omega_0 = -1.8$.

Another type of sensitivity study is shown in Fig. 6. Here, we consider peeling modes with higher mode numbers ($m/n = 12/2$ and $m/n = 18/3$) in Fig. 6(a). The safety factor $q = 6.05$ is fixed, which gives us fluid-wise stable peeling modes with $m/n = 6/1$, $m/n = 12/2$, and $m/n = 18/3$. In these calculations, the re-normalized frequency $\Omega = (\omega - n\omega_0)/n\omega_{ds}$ has been used in Eq. (17). A robust destabilization of the modes is obtained, at sufficiently high pressure of EPs. We also consider peeling modes with higher poloidal mode numbers ($m/n = 10/1$ and $m/n = 15/1$) while fixing the toroidal mode number. The results are shown in Fig. 6(b). In order to have fluid-wise stable peeling modes, $q = 10.05$ *and* $q = 15.05$ are chosen for the cases of $m/n = 10/1$ and $m/n = 15/1$, respectively. Stable peeling modes with higher poloidal mode numbers can also be destabilized by trapped EPs, as the EPs' pressure exceeds threshold values β_c^* that depend on the mode number. Generally, at the marginal stability point $\delta W_{k0} \approx \mathrm{Re}(\delta W_{k0}) \sim -\delta W_f^\infty$. Here, δW_f^∞ is determined by m/n and safety factor q. But $\mathrm{Re}(\delta W_{k0})$ displays a complicated dependence on the poloidal mode number through the terms shown in Eqs. (17)–(23). Consequently, the critical value β_c^* for destabilizing peeling mode is also a complicated function of the poloidal mode number. It is noteworthy that the predicted numbers for the threshold EPs' pressure, for destabilizing peeling modes, should not be taken too quantitatively, due to quite a few simplifying assumptions in the calculations. This work mainly provides qualitative conclusions.

Physically, a peeling mode with higher m is more localized near the plasma edge as shown in Fig. 7. This leads to less interaction between the trapped EPs and the mode in the configuration space. Indeed, we realize that δW_{k0} is eventually the radial integration of the product of the perpendicular displacement of the mode, with the gradient of the kinetic perturbed EPs' pressure.

IV. DESTABILIZATION OF IDEAL KINK-PEELING MODE BY EPs

In this section, we place a wall at the radial position of $b = 1.3a$. We consider a plasma with vanishing toroidal

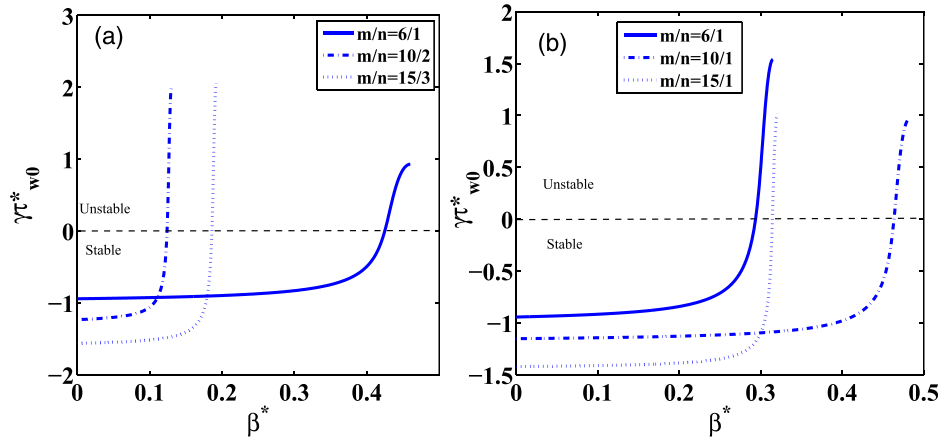

FIG. 6. (a) The growth/damping rates of the resistive-wall peeling modes, with $m/n = 6/1$(solid line), $m/n = 12/2$(dashed-dotted line), and $m/n = 18/3$(dotted line), respectively, as functions of the normalized pressure of EPs, β^*. $q = 6.05$ is used for all three cases. The particle pitch angle of $\lambda_0 = 1.43$ is chosen to allow destabilization of the resistive-wall peeling mode for all three cases. Here, τ^*_{w0} is the typical wall time corresponding to $m = 6$. The other parameters set as in Fig. 2 are used; (b) the growth/damping rates of the modes, with $m/n = 6/1$(solid line), $m/n = 10/1$(dashed-dotted line), and $m/n = 15/1$(dotted line), respectively, as functions of β^*. The particle pitch angle of $\lambda_0 = 1.3$ is chosen. The safety factor values of $q = 10.05$ and $q = 15.05$ are chosen for the cases of $m = 10$ and $m = 15$, respectively.

flow. A plasma with a finite rotation, as that studied in Sec. III, does not change the qualitative results shown here. The other parameters are the same as those specified at the beginning of Sec. III. This results in the fluid potential energy of $\delta W_f^b = 0.00301$ and $\delta W_f^\infty = 0.00300$. The fact that $\delta W_f^b \approx \delta W_f^\infty$ implies that the ideal (resistive) wall has negligible effect on the stability of the peeling mode. In this case, the eigenvalue of the kink-peeling mode is determined by the dispersion relation (11), which we numerically solve.

Figure 8 shows the growth/damping rate and the real frequency of the mode as functions of β^*. At $\beta^* = 0$ ($\delta W_{k0} = 0$), Eq. (11) has a pair of complex roots sharing the same growth rate $\gamma(= 0)$. The normalized real frequencies are $\Omega_r = \pm[(\delta W_p + \delta W_v^\infty)/\delta K]^{1/2}$, labeled by symbols "o" in Fig. 8(b). At finite β^*, another root of Eq. (11) appears,

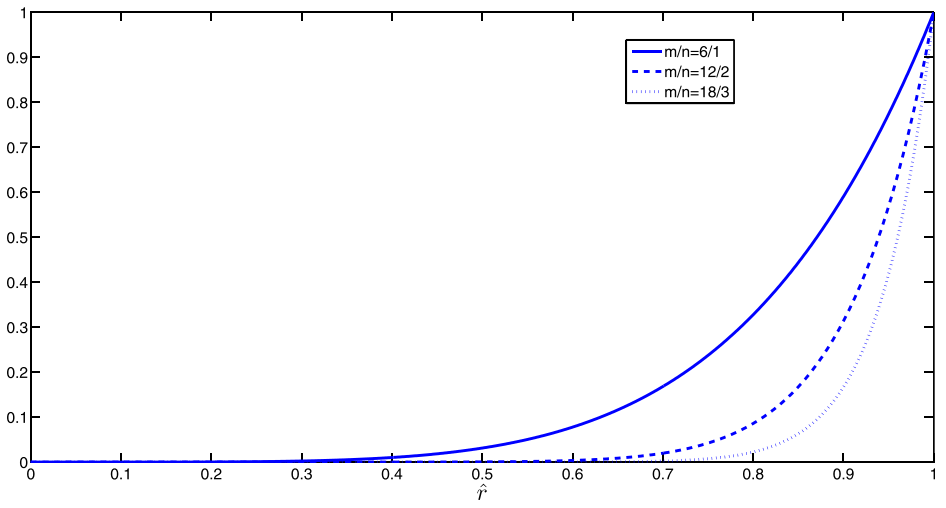

FIG. 7. The eigenfunctions (normalized radial displacement) of the peeling modes with $m/n = 6/1$, $m/n = 12/2$, and $m/n = 18/3$, respectively, used for computing the perturbed drift kinetic energy due to trapped EPs.

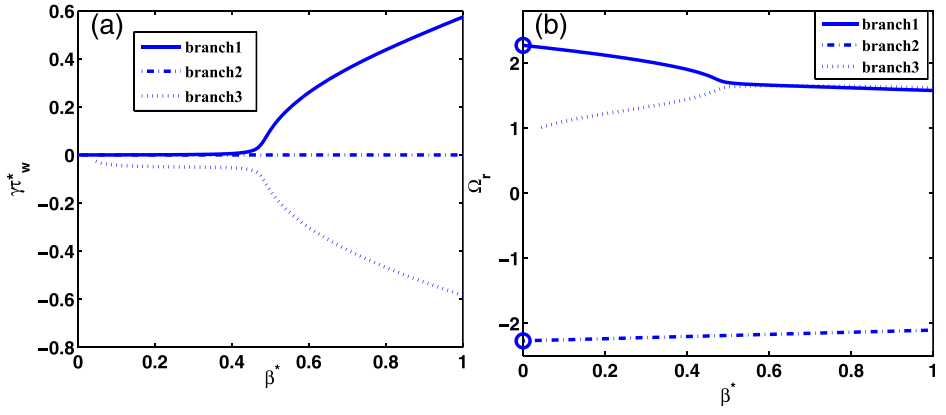

FIG. 8. (a) The normalized growth/damping rates ($\gamma\tau^*_w$) and (b) the normalized real frequency (Ω_r), of the ideal-kink peeling mode, as a function of the EPs' pressure β^*. Other parameters are $\lambda_0 = 1.05$, $\Omega_0 = 0$, and $b = 1.3a$.

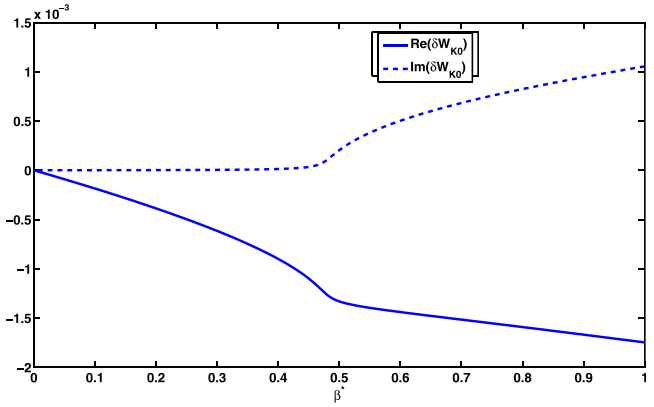

FIG. 9. The imaginary part $\mathrm{Im}(\delta W_{k0})$ (dashed curve) and the real part $\mathrm{Re}(\delta W_{k0})$ (solid line) of the perturbed drift kinetic energy, as functions of the EPs' pressure β^*, corresponding to the destabilized branch (branch 1) in Fig. 8.

labeled by branch 3 in Fig. 8(a). This root results from the non-linear dependence of the drift kinetic energy δW_{K0} on the mode eigenvalue. At small β^*, the growth rate of branch 1 is almost not affected by trapped EPs, but its real frequency decreases with increasing β^*. As β^* approaches a threshold value of $\beta_c^* = 0.58$, the growth rate rapidly increases with β^*. The marginal stable branch 1 becomes unstable. In the region near $\beta^* > 0.46$, two complex frequencies (branch 1 and branch 3) form a pair of complex conjugates, sharing the same real frequency Ω_r. The other branch, branch 2, is always stable, and is hardly affected by EPs. This branch can be labeled as the plasma mode in the conventional RWM theory. The above calculation mainly provides a qualitative conclusion that the ideal kink-peeling mode can be driven by trapped EPs.

Further calculations show that the appearance of an unstable branch of Eq. (11), as well as the critical value of β^* for destabilizing the kink-peeling mode, is not sensitive to the plasma rotation and to the wall position $b(>1.3a)$.

Figure 9 displays the energy analysis for the branch 1 (the destabilized branch) from Fig. 8. The $\mathrm{Re}(\delta W_{k0})$ is negative. Its amplitude is roughly proportional to β^*, leading to a decrease of the mode rotation frequency Ω_r with increasing β^*, as shown in Fig. 8. The decrease of Ω_r in turn results in an increase of γ as indicated by Eq. (12). The coupling between the real and imaginary part of the mode eigenvalue is of course non-linear. The full eigenvalue eventually affects $\mathrm{Im}(\delta W_{k0})$ through the log-functions in Eqs. (18)–(20). This non-linear coupling of the eigenvalue via the drift kinetic energy component predicts the destabilization of an unstable kink-peeling mode by trapped EPs.

V. CONCLUSION

The drift kinetic effects of EPs on the stability of edge localized, high-m peeling modes are investigated using an analytic MHD-drift kinetic hybrid formulation similar to that for the RWM. This formulation is based on the extended kinetic energy principle. Depending on the wall distance to the plasma boundary, either a resistive-wall peeling mode or an ideal-kink peeling mode is considered.

With a close-fitting resistive wall, the peeling mode is essentially a RWM, which has a low n and high m mode numbers. This resistive-wall peeling mode is described by the kinetic RWM dispersion relation neglecting the plasma inertial effect. The radial profile of the mode eigenfunction peaks near the plasma edge as m becomes large. We find that a resistive-wall peeling mode, which is stable in the fluid approximation (i.e., without the kinetic effects from EPs), can be destabilized by trapped EPs with a slowing down distribution in the particle energy space and a δ-function distribution in the particle pitch angle. The destabilization comes from both the mode–particle resonance and the non-resonance part of EPs' contribution.

A resistive wall farther from the plasma boundary has negligible effect on the edge localized peeling mode. In this case, the plasma inertia becomes important, and we consider an ideal-kink peeling mode. This mode can also be driven unstable by trapped EPs.

The above results indicate that the destabilization of the edge localized peeling mode (either resistive-wall peeling or ideal-kink peeling) by EPs is rather robust. This may offer an explanation of the (robust) observation of the ELM triggering by EP driven mode (EPdM) observed in JT-60U and DIII-D. The trapped EPs are transported to the plasma edge by EPdM, and then, these EPs can destabilize new branch (low-n peeling mode) which can trigger ELM in the same way as usual ELM.[14,29] It is noteworthy that the predicted numbers for the threshold EPs' pressure, for destabilizing peeling mode, should not be taken too quantitatively, due to quite a few simplifying assumptions in the calculations. This work mainly provides qualitative conclusions. A more quantitative investigation of the EP-driving peeling mode is underway using the full toroidal MHD-kinetic hybrid code MARS-K.[24]

ACKNOWLEDGMENTS

This work was supported by National Natural Science Foundation of China under Grant No. 11205051 and also supported by National Magnetic Confinement Fusion Science Program under Grant Nos. 2009GB101002 and 2010GB106006. This work was part-funded by the RCUK Energy Programme under Grant No. EP/I501045 and the European Communities under the contract of Association between EURATOM and CCFE. The views and opinions expressed herein do not necessarily reflect those of the European Commission. G. Z. Hao acknowledges the hospitality of Euratom/CCFE Fusion Association, where part of the work was completed.

[1]J. A. Wesson, Nucl. Fusion **18**, 87 (1978).
[2]J. W. Connor, R. J. Hastie, H. R. Wilson, and R. L. Miller, Phys. Plasmas **5**, 2687 (1998).
[3]D. Lortz, Nucl. Fusion **15**, 49 (1975).
[4]F. Wagner *et al.*, Phys. Rev. Lett. **49**, 1408 (1982).
[5]J. Manickam, Phys. Fluids B **4**, 1901 (1992).
[6]G. T. A. Huysmans, T. C. Hender, and B. Alper, Nucl. Fusion **38**, 179 (1998).
[7]C. P. Perez *et al.*, Nucl. Fusion **44**, 609 (2004).
[8]C. G. Gimblett, R. J. Hastie, and P. Helander, Phys. Rev. Lett. **96**, 035006 (2006).

[9]P. B. Snyder *et al.*, Nucl. Fusion **47**, 961 (2007).
[10]Y. Q. Liu, S. Saarelma, M. P. Gryaznevich, T. C. Hender, D. F. Howell, and JET-EFDA Contributors, Plasma Phys. Controlled Fusion **52**, 045011 (2010).
[11]S. Y. Medvedev, A. Degeling, Y. Martin, O. Sauter, and L. Villard, in *30th European Conference on Controlled Fusion and Plasma Physics* (St. Petersburg, 2003), Vol. 27A, pp. 3–129.
[12]G. T. A. Huysmans, Plasma Phys. Controlled Fusion **47**, 2107 (2005).
[13]A. J. Webster and C. G. Gimblett, Phys. Rev. Lett. **102**, 035003 (2009).
[14]G. Matsunaga *et al.*, in *Proceedings of the 24th IAEA Fusion Energy Conference 2012, San Diego, USA, 2012* (IAEA, Vienna, 2012), EX/5–1.
[15]G. Z. Hao, A. K. Wang, Y. Q. Liu, and X. M. Qiu, Phys. Rev. Lett. **107**, 015001 (2011).
[16]B. Hu and R. Betti, Phys. Rev. Lett. **93**, 105002 (2004).
[17]M. S. Chu, J. M. Greene, T. H. Jensen, R. L. Miller, A. Bondeson, R. W. Johnson, and M. E. Mauel, Phys. Plasmas **2**, 2236 (1995).
[18]G. Z. Hao, Y. Q. Liu, A. K. Wang, and X. M. Qiu, Phys. Plasmas **19**, 032507 (2012).
[19]G. Z. Hao, Y. Q. Liu, A. K. Wang, H. B. Jiang, G. M. Lu, H. D. He, and X. M. Qiu, Phys. Plasmas **18**, 032513 (2011).
[20]Y. Q. Liu, M. S. Chu, C. G. Gimblett, and R. J. Hastie, Phys. Plasmas **15**, 092505 (2008).
[21]B. Hu, R. Betti, and J. Manickam, Phys. Plasmas **12**, 057301 (2005).
[22]J. P. Freidberg, *Ideal Magnetohydrodynamics* (Clarendon, Oxford, 1987).
[23]S. W. Haney and J. P. Freidberg, Phys. Fluids B **1**, 1637 (1989).
[24]Y. Q. Liu, M. S. Chu, I. T. Chapman, and T. C. Hender, Phys. Plasmas **15**, 112503 (2008).
[25]V. D. Shafranov, Sov. Phys. Tech. Phys. **15**, 175 (1970).
[26]J. Wesson, *Tokamaks* (Clarendon Press, Oxford, 2004).
[27]R. B. White, L. Chen, F. Romanelli, and R. Hay, Phys. Fluids **28**(1), 278 (1985).
[28]R. Takahashi, D. P. Brennan, and C. C. Kim, Nucl. Fusion **49**, 065032 (2009).
[29]G. Matsunaga, K. Shinohara, N. Aiba, Y. Sakamoto, A. Isayama, N. Asakura, T. Suzuki, M. Takechi, N. Oyama, H. Urano, and the JT-60 Team, Nucl. Fusion **50**, 084003 (2010).